

Differentiating pathogenic from bystander autoantibodies in immune thrombocytopenia using intact glycoprotein-deficient megakaryocytes

by Nanyan Zhang, Günel Uzun, Tamam Bakchoul, Brian R. Curtis and Peter J. Newman

Received: July 29, 2025.

Accepted: December 5, 2025.

Citation: Nanyan Zhang, Günel Uzun, Tamam Bakchoul, Brian R. Curtis and Peter J. Newman. Differentiating pathogenic from bystander autoantibodies in immune thrombocytopenia using intact glycoprotein-deficient megakaryocytes.

Haematologica. 2025 Dec 11. doi: 10.3324/haematol.2025.288832 [Epub ahead of print]

Publisher's Disclaimer.

E-publishing ahead of print is increasingly important for the rapid dissemination of science.

Haematologica is, therefore, E-publishing PDF files of an early version of manuscripts that have completed a regular peer review and have been accepted for publication.

E-publishing of this PDF file has been approved by the authors.

After having E-published Ahead of Print, manuscripts will then undergo technical and English editing, typesetting, proof correction and be presented for the authors' final approval; the final version of the manuscript will then appear in a regular issue of the journal.

All legal disclaimers that apply to the journal also pertain to this production process.

Differentiating pathogenic from bystander autoantibodies in immune thrombocytopenia using intact glycoprotein-deficient megakaryocytes

Nanyan Zhang¹, Günalp Uzun², Tamam Bakchoul², Brian R. Curtis¹, Peter J. Newman^{1,3,4}

¹Versiti Blood Research Institute, Milwaukee, WI, USA

²Institute for Clinical and Experimental Transfusion Medicine, University Hospital Tübingen; Tübingen, Germany

³Departments of Pharmacology and ⁴Cell Biology, Medical College of Wisconsin; Milwaukee, WI, USA

Corresponding author: Nanyan Zhang, Blood Research Institute, Versiti Blood Center of Wisconsin, 8727 Watertown Plank Rd, Milwaukee, WI 53226; email: nzhang@versiti.org

Running head: iPSC-derived autoantigen-deficient megakaryocytes

Data-sharing statement: For original data, please contact nzhang@versiti.org.

Author contributions: N.Z. conducted experiments and analyzed data. G.U. and T.B. provided MAIPA-tested ITP patient plasma and helped interpret data. B.R.C. provided PABA- and ELISA-tested ITP patient plasma and helped interpret data. N.Z. and P.J.N. designed experiments and wrote the manuscript.

Acknowledgments: We thank Dr. Taisuke Kanaji at the Scripps Research Institute for providing the pCDNAzeo-hGPIb α pro-hIL4R α -GPIb α plasmid, and Dr. Maria Therese Ahlen at the University Hospital of North Norway for providing anti-HPA-1a (26.4) alloantibody.

Disclosures:

B.R.C. is a consultant for Rallybio in the field of platelet alloimmunity. The remaining authors declare no competing financial interests.

Funding: National Heart Lung and Blood Institute of the National Institutes of Health grant R35 HL139937 (PJN)

Text word count: 3808 **Abstract word count:** 173 **Figure count:** 4 **Supplementary file:** 1

Declaration of AI-assisted technologies

During the preparation of this work, the authors used ChatGPT-4o to enhance the readability and language of several sections of the manuscript. All content was subsequently reviewed and edited by the authors, who take full responsibility for the final version of the published article.

Abstract:

Autoantibodies targeting platelet surface glycoproteins (GP) are the primary cause of immune thrombocytopenia (ITP), however testing for these autoantibodies is not routinely employed mainly because current diagnostic tests lack sufficient sensitivity. To overcome this and other diagnostic limitations, we generated HLA Class I-negative, blood group O, induced pluripotent stem cell lines, and gene-edited them to produce a novel panel of GP-deficient, *in vitro*-derived megakaryocytes (MK). Using GPIIb-, GPIb α - and GPIX-deficient MK allowed sensitive and specific identification and characterization of both GPIIb-IIIa- and GPIb/IX-specific plasma autoantibodies, as well as rare, previously undescribed patient autoantibodies targeting GPIX. The availability of frozen bioengineered MK expressing select platelet glycoprotein antigens on their surface simplifies the detection of anti-platelet autoantibodies involved in disease progression, while avoiding detection of non-pathogenic bystander autoantibodies that are sometimes generated by secondary exposure to “cryptic epitopes”, and that can otherwise confound diagnosis and treatment. Use of intact MK selectively deficient in the glycoproteins that comprise the major targets of platelet autoantibodies has the potential to significantly improve clinical diagnosis and treatment of ITP.

INTRODUCTION

Immune thrombocytopenia (ITP) is an autoimmune disorder primarily characterized by a low platelet count. Many patients have few or only mild bleeding symptoms, but severe and life-threatening bleeding may occur and sometimes requires extensive, long-term care that can compromise the health-related quality of life.¹ Even today, ITP remains a diagnosis of exclusion, due to the lack of reliable standard tests or biomarkers to confirm diagnosis. Nearly 1 in 7 patients with primary ITP are misdiagnosed,² with significant implications for ITP management, and may expose patients to unnecessary treatment. Platelet autoantibodies are the primary drivers of ITP, although other mechanisms, such as cytotoxic T cells and natural killer cells, may also contribute to ITP pathogenesis. Despite their central role, platelet autoantibody tests are not routinely employed for diagnosing ITP mainly due to the low sensitivity of existing methods. Thus, while a positive autoantibody test is useful for confirming ITP, a negative test does not rule it out.³ Therefore, there is a critical need for alternative, practical methods that can detect anti-platelet autoantibodies with high specificity and sensitivity to provide a positive laboratory confirmation for the diagnosis of ITP.

Platelet surface glycoproteins (GP), primarily GPIIb-IIIa and GPIb/IX, are the major targets of anti-platelet autoantibodies causing ITP.⁴⁻⁶ Subsequent clearance of opsonized platelets is largely mediated through Fcγ receptor-dependent phagocytosis, or via platelet desialylation mechanisms.⁷ Uncertainty regarding the relationship between autoantibody specificity, the mechanism of platelet destruction and the response to certain treatments, however, has limited the usefulness of diagnostic testing for ITP, and is therefore often not even prescribed.⁸⁻¹⁷ Currently, antigen capture assays (ACA) like enzyme-linked immunosorbent assay (ELISA),¹⁸ monoclonal antibody-specific immobilization of platelet antigens (MAIPA)¹⁹ and platelet antibody bead array (PABA)²⁰ are favored in clinical diagnostic laboratories for their glycoprotein specificity. However, they are labor-intensive and employ detergents to solubilize platelet glycoproteins, which may destroy labile epitopes. Monoclonal antibodies used in these assays may also compete with the binding of anti-platelet autoantibodies, resulting in false negative outcomes. Additionally, these tests are often conducted only in specialized laboratories, each setting their own threshold for positivity. Even minor differences in these threshold values can affect the detection of weak or low-affinity autoantibodies, potentially causing false negative or false positive results.

Regardless of the assay used, platelet autoantibodies can be derived from two sources: antibodies bound to the patient's platelets, and free-circulating antibodies present in the patient's plasma. Diagnostic laboratories typically prefer, when possible, to obtain platelet-associated antibodies by eluting them from patient platelets, as this approach is more sensitive due to the enrichment of autoantibodies on the cell surface. However, this method requires a substantial blood volume and an adequate platelet count, which may not be feasible in patients with severe thrombocytopenia. In such cases, detection of circulating plasma antibodies, though less sensitive, is often the only viable option. Analyzing plasma autoantibodies also holds significant value in research, as plasma samples from ITP patients serve as important resources for studying disease pathogenesis, prognosis, and treatment response. Unlike platelet-associated antibodies that target only extracellular domains of platelet glycoproteins, plasma may contain antibodies against intracellular epitopes.^{21, 22} While these intracellular-targeting antibodies are not thought

to be pathogenic, they may arise as a secondary immune response in the context of platelet destruction, and have the potential to confound both diagnosis and treatment.

Assays based on the use of intact platelets were developed long ago to detect platelet-specific antibodies. By preserving intact, native surface antigens, these assays offer high sensitivity. However, they were ultimately abandoned for ITP autoantibody detection due to poor specificity, stemming from the complex array of antigens expressed on the platelet surface. Reliable detection of ITP autoantibodies using intact platelets has only been achieved in rare cases—typically when glycoprotein-deficient donor platelets from individuals with Glanzmann's thrombasthenia or Bernard-Soulier syndrome (BSS) served as negative controls.^{4, 23} In addition to platelet-specific antigens, platelets also express ABO blood group antigens and HLA class I molecules, which further complicate the interpretation of antibody specificity.

In the current study, we aimed to revive the whole-cell assay for detecting ITP autoantibodies in patient plasma by replacing donor-derived platelets with bioengineered megakaryocytes (MK), achieving high sensitivity and exceptional specificity. By creating GP-knockout (KO) induced pluripotent stem cell (iPSC)-derived MK, we were able to sensitively detect and accurately characterize autoantibodies against major platelet surface GP complexes, namely GPIIb-IIIa and GPIb/IX, including those previously undetectable by standard ACA. Moreover, the use of GPIIb KO and GPIX KO MK enabled detection of a previously undescribed anti-GPIX autoantibody, demonstrating enhanced resolution for autoantibody characterization. Importantly, the use of intact MK avoids detecting non-pathogenic 'innocent bystander' autoantibodies in patient sera that are detectable using standard ACAs. The ready availability of frozen bioengineered MK should streamline the detection of anti-platelet autoantibodies, thus significantly enhancing the research and the clinical diagnosis and treatment of ITP.

METHODS

Study design

The use of deidentified ITP patient plasma samples was approved by the Medical College of Wisconsin/Froedtert Hospital Institutional Review Board (PRO00036374). Patient consent was waived in accordance with the approved IRB protocol. Patient plasma samples were obtained from two clinical diagnostic laboratories: the Platelet and Neutrophil Immunology Laboratory at Versiti, Wisconsin (Site 1), and the Institute for Clinical Immunology and Transfusion Medicine at the University Hospital of Tübingen, Germany (Site 2). To ensure the inclusion of true ITP cases, only samples from patients previously confirmed to have platelet-associated or circulating antibodies were selected by the diagnostic laboratories. Twenty-eight ITP plasma samples from Site 1 had been previously tested using diagnostic PABA²⁰ or ELISA¹⁸, while 20 samples from Site 2 had been tested using diagnostic MAIPA¹⁹. All ITP patient samples were blinded and coded by the diagnostic laboratories before being transferred to the research laboratory for testing using intact MK. As negative quality control, twenty deidentified normal human plasma samples obtained from Versiti were pooled and included in each test. Additionally, Site 1 provided three coded normal plasmas randomized among the ITP samples to ensure assay

accuracy. Diagnostic test results were released subsequently by the laboratories for comparative analysis and are summarized in *Supplementary Table S1*.

Flow cytometric analysis

To analyze MK surface glycoprotein expression, 2×10^5 cells were incubated with the following fluorescently conjugated antibodies at room temperature for 20 min: PE/Cyanine7-conjugated anti-GPIIb, FITC-conjugated anti-GPIIIa, APC-conjugated anti-GPIb α (BioLegend), PE-conjugated anti- α V β 3, clone LM609 (Sigma), AF647-conjugated anti-GPVI (11A12), FITC-conjugated anti-GPIX (BD Biosciences), Alexa Fluor 488-conjugated anti-IL-4R α (R&D systems). Fluorescently labeled isotype controls corresponding to each monoclonal antibody were included as background staining. GPV surface expression was monitored by incubating the MK with sheep anti-GPV primary antibody (R&D systems) followed by Alexa Fluor 488-conjugated donkey anti-sheep IgG (Jackson ImmunoResearch Laboratories). For autoantibody detection (*Supplementary Figure S1*), 5×10^5 iPSC-derived MK were incubated with 10-25 μ l of human plasma for 30 min at room temperature. After washing, the cells were incubated with PE-conjugated donkey anti-human IgG (Jackson ImmunoResearch Laboratories), PE/Cyanine7-conjugated anti-GPIIb, and either APC-conjugated anti-GPIb α or AF647-conjugated anti-GPVI at room temperature for 20 min. Cells not exposed to human plasma, but stained with secondary and gating antibodies, served as negative controls. Anti-HPA-1a (26.4) alloantibody, a kind gift from Dr. Maria Therese Ahlen (University Hospital of North Norway), was used as a positive control. Flow cytometry was performed using a BD FACSCelesta or FACSymphony A5 SE cell analyzer. Data were analyzed using FlowJo software (Tree Star Inc.). Flow cytometry data were visualized on a biexponential scale. Due to digital background subtraction, some fluorescence intensity values for unstained populations were negative; these values were considered background noise.

Statistical analysis

Statistical tests were performed using GraphPad Prism 9 (GraphPad Software). Analysis between multiple groups was performed using one-way ANOVA with Dunnett's test for comparison between individual groups. $P < 0.05$ was considered statistically significant.

RESULTS

Generation and characterization of GPIIb-IIIa- and GPIb/IX-deficient iPSC lines

A blood group O, HLA class I-negative iPSC line²⁴ was used as the founder line for all gene-editing procedures because its differentiated megakaryocytes exhibited low background binding to plasma from 21 randomly selected healthy donors (*Supplementary Figure S2*). iPSC clones in which the gene encoding platelet membrane GPIIb was deleted were then generated using CRISPR/Cas9 technology (*Supplementary Figure S3A*). Disruption of the GPIIb gene did not affect differentiation of iPSC into MK, and the size of GPIIb KO MK was comparable to that of wild-type (WT) MK (*Supplementary Figure S4*). Flow cytometric analysis confirmed the complete loss of GPIIb surface expression (Figure 1A). As expected, GPIIb-deficiency also resulted in a significant reduction in MK surface expression of GPIIIa; the remaining low level

of GPIIIa is due to rescue of its expression by an endogenous integrin αV subunit and formation of $\alpha V\beta 3$ (Figure 1A). Disruption of GPIIb did not affect the expression of other major glycoproteins, such as GPIb α and GPVI, on the MK surface (Figure 1A).

The GPIb/IX/V complex is comprised of a large GPIb α subunit disulfide linked to GPIb β and noncovalently associated with GPIX and GPV.²⁵ We generated GPIb α , GPIX and GPV single knockout iPSC clones (*Supplementary Figure S3B-D*), and also introduced a transgene encoding a chimeric IL4R α -GPIb α ²⁶ protein into the AAVS1 locus of the GPIb α KO iPSC clone (*Supplementary Figure S5*). This fusion protein, depicted on the left side of Figure 1B, replaces almost the entire extracellular domain of human GPIb α with the extracellular domain of human interleukin-4 receptor α (IL4R α). IL4R α -GPIb α has previously been shown to associate with GPIb β in a manner mimicking the intact GPIb α subunit, and fully supports assembly of the GPIb/IX complex.²⁶ Wild-type iPSC clones were then differentiated into MK, and found to express high levels of GPIb α , GPIX and GPV on the cell surface (Figure 1B). In contrast, GPIb α -deficient MK completely lost GPIb α expression, and also exhibited significantly reduced surface GPIX and GPV expression (Figure 1B), as expected. Similarly, GPIX-deficient MK showed significantly reduced levels of GPIb α and GPV (Figure 1B). In contrast, GPV-deficient MK expressed normal levels of GPIb α and GPIX (Figure 1B), consistent with previous findings that GPV biosynthesis and surface expression depend on the presence of GPIb/IX complex, but GPIb/IX surface expression doesn't require GPV.^{27, 28} Expression of IL4R α -GPIb α restored GPIX surface expression in GPIb α -deficient MK, as expected, but only partially restored expression of GPV (Figure 1B), suggesting that interaction with the extracellular domain of GPIb α may play an important role in trafficking GPV to the cell surface. Finally, targeted disruption of GPIb/IX/V did not significantly affect the expression of other major glycoproteins, such as GPIIb and GPVI (Figure 1B).

Identification of glycoprotein-specific autoantibodies from ITP plasmas using bioengineered megakaryocytes

As shown in Figure 2A, ITP patient plasmas 1-4, previously typed using diagnostic ACA (*Supplementary Table S1*), showed strong binding to both WT MK and GPIb α KO MK. Patients 1 and 2 completely lost binding to GPIIb KO MK, suggesting that the autoantibodies target either GPIIb or elsewhere on the GPIIb-IIIa complex, while plasmas from patients 3 and 4 showed significantly decreased, but not negative, binding to GPIIb KO MK, suggesting the autoantibodies are highly likely targeting the GPIIIa ($\beta 3$) subunit, which remains expressed in $\alpha V\beta 3$ complex on GPIIb KO MK. Supporting this notion, a GPIIIa specific *allo*antibody (anti-HPA-1a)²⁹ demonstrated a similarly low levels of binding to GPIIb KO MK. Notably, the use of whole intact MK also allowed detection of ITP patient antibodies from the plasmas previously undetectable using standard diagnostic ACA methods. For example, plasma samples from ITP patients 5-8, which tested negative in the ACA (*Supplementary Table S1*), exhibited various degrees of binding to both WT and GPIb α KO MK, but did not react with GPIIb KO MKs (Figure 2B), consistent with the notion that autoantibodies in these patients target so-called “labile epitopes” that become disrupted during detergent solubilization procedures commonly used in ACA. Additionally, blocking Fc γ RIIa receptors with anti-Fc γ RIIa antibody IV.3 did not affect ITP autoantibody binding to MKs, demonstrating that nonspecific antibody binding via

FcγRIIIa receptor did not play a role in this autoantibody detection system (*Supplementary Figure S6*).

ITP patient plasmas containing confirmed anti-GPIIb/IX autoantibodies were also examined for their ability to react with iPSC-derived MK. As shown in Figure 3A, plasma from patients 9, 11, and 12 exhibited varying degrees of binding to both WT and GPIIb KO MK, but lost reactivity with GPIbα KO and GPIX KO MK, indicating the presence of antibodies targeting the GPIb/IX complex. Patient 10 showed strong binding to WT, GPIbα KO, and GPV KO MK, but markedly reduced binding to GPIIb KO and GPIX KO MK, suggesting the coexistence of anti-GPIIb-IIIa and anti-GPIX autoantibodies (Figure 3A). Notably, this case highlights the enhanced resolution provided by the MK panel, enabling the identification of a previously unrecognized anti-GPIX autoantibody in patient 10. Although anti-GPIIb-IIIa autoantibodies were also detected in patients 11 and 12 by ACA, their presence could not be confirmed using the whole MK panel.

Similar to the findings with GPIIb-IIIa-specific autoantibodies, the MK panel also detected plasma autoantibodies against the GPIb/IX complex that were not identified by ACA. Plasma from patients 13 to 15 exhibited strong binding to WT MK, markedly reduced binding to GPIIb KO MK, and moderately reduced binding to GPIbα KO and GPIX KO MK (Figure 3B), suggesting the coexistence of a strong anti-GPIIb-IIIa antibody and a weaker anti-GPIb/IX antibody in these samples. Patient 16 demonstrated strong antibody binding to WT MK, with significantly reduced binding to GPIIb KO, GPIbα KO, and GPIX KO MKs, indicating the presence of both strong anti-GPIIb-IIIa and anti-GPIb/IX autoantibodies (Figure 3B). Collectively, these results provide compelling evidence for the ability of iPSC-derived, glycoprotein-deficient MK to both detect and characterize ITP antibodies with increased sensitivity and resolution – qualities that could be of future importance in directing therapy (see Discussion). As expected, this whole-cell assay is also applicable for detecting anti-platelet isoantibodies, as demonstrated by the successful identification of a previously missed anti-GPIb/IX antibody in a BSS patient with suspected anti-platelet antibodies following blood transfusion (*Supplementary Figure S7*).

Discrimination of non-membrane-reactive autoantibodies from pathogenic antibodies causing platelet destruction

As shown in *Supplementary Table S1*, a total of 48 ITP patient plasma samples were tested with whole megakaryocytes (WMK) in this study—28 from Site 1 and 20 from Site 2. Although different ACA methods were used by the two diagnostic laboratories, the results could be categorized into three groups, as illustrated in Figure 4A. WMK confirmed the diagnostic ACA findings in 46.4% and 44.4% of cases from Site 1 and Site 2, respectively. Notably, WMK identified previously undetectable autoantibodies in 21.4% of samples from Site 1 and 22.2% from Site 2, underscoring the advantage of preserving labile native antigens in these cases. Importantly, autoantibodies in 32.1% (Site 1) and 33.3% (Site 2) of samples were not detected by WMK, raising concerns that some laboratory ACA results may be misleading and highlighting the need for further evaluation and cautious clinical interpretation.

Previous studies have shown the existence in the plasmas of ITP patients of antibodies that bind the cytoplasmic domains of platelet membrane glycoproteins,^{21,22} and although detected by

some ACA-type assays, have little to do with the pathology of ITP because they do not bind to or mediate the clearance of intact cells. In this regard, the use of bioengineered MK provides an advantage by only reporting the presence of those autoantibodies capable of actually binding to and removing platelet from circulation. As a case in point is demonstrated in Figure 4, in which ITP plasma from patient 17 was found to react strongly with GPIb/IX in diagnostic ACA (Figure 4B), while showing little reactivity with intact iPSC-derived MK (Figure 4C) and intact human platelets (*Supplementary Figure S8*), suggesting that the detected antibody is non-pathogenic and likely represents a bystander in the patient's plasma. Such ACA results may be misleading, particularly when platelet-associated antibody testing cannot be performed due to severe thrombocytopenia, as was the case for this patient (*Supplementary Table S1*). To further investigate the nature of this antibody and localize its epitope, we performed a modified ACA using WT MK or IL4R α -GPIb α MK expressing a chimeric protein lacking the GPIb α extracellular domain (Figure 4D). The antibody bound to the wild-type GPIb/IX complex but failed to bind the chimeric protein complex, indicating that its epitope is located on or associated with a cryptic region of the GPIb α extracellular domain. While the mechanisms by which such cryptic epitopes are exposed in ACA-type assays remain unclear, these findings underscore the value of using intact bioengineered, glycoprotein-deficient iPSC-derived MK as reliable tools for identifying pathogenic autoantibodies in ITP.

ITP is a heterogeneous disorder. Although the presence of bystander antibodies detected by ACA may explain some cases that were negative in WMK but positive in ACA (Figure 4A), this alone may not account for all instances, and other explanations are possible. First, ACAs may in some cases be more sensitive than flow cytometry–based whole-cell assays, as they present a higher density of target antigens on beads or microplate surfaces. This may be particularly relevant for autoantibodies that recognize linear peptide epitopes or conformational epitopes that remain stable during platelet solubilization. Second, we cannot fully exclude the possibility that certain disease-relevant epitopes are absent or underrepresented in iPSC-derived megakaryocytes, although these cells demonstrated robust binding to multiple well-characterized monoclonal antibodies against diverse epitopes on GPIIb-IIIa and GPIb α .

DISCUSSION

Identification of antiplatelet autoantibodies that are clinically relevant to the pathology of ITP has historically been constrained by the relatively low sensitivity and specificity of the diagnostic tests commonly used to detect them. The major contribution of the present investigation is the development and use of intact iPSC-derived megakaryocyte cell lines lacking selected platelet membrane glycoprotein autoantibody targets (*Supplementary Figure S1*). Combined with flow cytometric detection, these offer a number of unique advantages over existing ELISA-based methods.

Firstly, the use of intact cells expressing antigens in their native form on the cell surface improves detection of antibodies directed against labile antigens that become disrupted following platelet solubilization. Labile antigens have been reported for some hard-to-detect anti-platelet *allo*antibodies, including those specific for the human platelet alloantigens (HPA)-3a, 3b, and 9b.^{24, 30-33} Detecting *auto*antibodies can be even more challenging than detecting *allo*antibodies

due to often low abundance and affinity of autoantibodies present in ITP patient plasma. Surprisingly, we found that many autoantibodies, undetectable in standard ELISA-based tests, showed strong binding to intact megakaryocytes (Figure 2B, 3B), providing additional evidence for ITP autoantibodies that target labile conformational antigens that become disrupted upon detergent solubilization.

Second, GP-deficient MK serve as their own internal controls, providing both enhanced specificity and increased resolution for autoantibody epitope characterization. For example, GPIb α is the only member of the GPIb/IX complex previously found to harbor autoreactive epitopes.³⁴ Using intact iPSC-derived megakaryocyte cell lines lacking carefully selected platelet membrane glycoproteins, however, we were able to identify an autoantibody with specificity for the GPIX component of this complex (Figure 3A) - a critical first step in the design of glycoprotein-specific chimeric autoantibody receptor (CAAR) T cells aimed at reducing the titer of circulating autoantibodies (c.f. reference³⁵ and discussion below).

Third, the use of intact cells restricts identification to only those autoantibody subpopulations able to react with cell surface epitopes, ignoring so-called bystander antibodies that can arise downstream of antibody-mediate platelet destruction. Such cryptic epitopes, often on the intracellular regions of platelet surface glycoproteins^{21, 22} or cytoplasmic proteins^{36, 37}, are generated as a secondary immune response, and have been found in both ITP as well as other platelet-destructive conditions like posttransfusion purpura and drug-induced immune thrombocytopenia.³⁸ Cryptic epitopes may also be located within the extracellular domains of platelet surface glycoproteins, and are exposed under conditions such as platelet aging, activation, or damage.³⁹⁻⁴² Naturally occurring autoantibodies to such epitopes are thought to help clear aged or damaged platelets from circulation.

Fourth, as platelet precursors, MK present a comprehensive array of platelet surface glycoprotein targets, thereby offering the potential to detect autoantibodies against rare antigens that are not included in ELISA-based testing panels. Autoantibodies targeting GPVI have been reported in some cases of ITP.⁴³⁻⁴⁶ Such cases are likely under-recognized since GPVI is not offered as a target in the current ITP testing panels. Although we have not generated GPVI-deficient MKs for antibody specificity characterization, we expect to detect currently unknown antibodies binding to the WT MK in initial screens. Further studies can then be conducted to address autoantigen specificity. Such an approach will reduce the possibility of missing potentially disease-causing autoantibodies.

The anti-CD20 monoclonal antibody, Rituximab, is often used as second-line therapy to eliminate B cells, independent of their specificity, for ITP treatment. Though initially developed for hematologic cancers, chimeric antigen receptor (CAR)-bearing T-cells directed against CD19 and CD20 are currently undergoing clinical trials for a number of autoimmune disorders.⁴⁷ Beginning in 2016, CAR T cells were repurposed to express chimeric *autoantigens* on their surface, facilitating specific elimination of pathogenic autoreactive B cells, while sparing B cells uninvolved in the autoimmune disease.⁴⁸⁻⁵⁰ In the ITP field, GPIb α -CAAR-T cells have been developed to eliminate GPIb α -specific B cells.³⁵ Future advancements may involve the development of a wide range of glycoprotein-specific CAAR-T cells, further highlighting the

need for sensitive assays such as the one described here that precisely identify targets of anti-platelet autoantibodies, crucial for selecting appropriate CAAR-T cells for ITP treatment.

ITP is a heterogeneous disorder comprising distinct groups of patients with varied clinical and serological profiles. Identifying pathogenic antiplatelet autoantibodies is critical for advancing our understanding of the disease and holds significant promise for improving ITP research, diagnosis, and treatment. As demonstrated in the current study, the whole megakaryocyte assay enables sensitive detection and characterization of pathogenic autoantibodies from ITP plasma. This approach could also be applied to analyze platelet-associated autoantibodies, provided they are eluted from patient platelets (*Supplementary Figure S9*). However, we were only able to conduct a pilot study to demonstrate feasibility, as additional patient platelets and eluates were not available.

Currently, ITP diagnosis relies on exclusion of other causes, which carries a risk of misdiagnosis. To mitigate this risk when working with deidentified plasma samples lacking full clinical histories, we included only patients previously confirmed to harbor platelet-associated or circulating autoantibodies. Future clinical studies incorporating both antibody-positive and antibody-negative ITP cases, together with complete patient medical histories, will be required to fully establish the clinical utility of the WMK assay. We anticipate that WMK may uncover missed antibodies in serologically unconfirmed ITP cases, analogous to our detection of a previously undetectable anti-GPIb/IX isoantibody in a patient with Bernard Soulier Syndrome (BSS) (*Supplementary Figure S7*), thereby enhancing the sensitivity and accuracy of ITP diagnosis.

The current glycoprotein-deficient megakaryocyte panel could be expanded to include additional glycoprotein targets, such as GPIa/IIa and GPVI. However, validation of these targets is currently limited by the lack of relevant ITP plasma samples from our diagnostic lab. A major challenge for clinical application of this novel strategy lies in producing sufficient quantities of megakaryocytes from established iPSC lines, as most diagnostic laboratories are not equipped to perform megakaryocyte differentiation. Future efforts to immortalize bioengineered iPSC-derived megakaryocytes may overcome this barrier and facilitate broader clinical implementation.

References

1. Efficace F, Mandelli F, Fazi P, et al. Health-related quality of life and burden of fatigue in patients with primary immune thrombocytopenia by phase of disease. *Am J of Hematol*. 2016;91(10):995-1001.
2. Arnold DM, Nazy I, Clare R, et al. Misdiagnosis of primary immune thrombocytopenia and frequency of bleeding: lessons from the McMaster ITP Registry. *Blood Adv*. 2017;1(25):2414-2420.
3. Vrbensky JR, Moore JE, Arnold DM, Smith JW, Kelton JG, Nazy I. The sensitivity and specificity of platelet autoantibody testing in immune thrombocytopenia: a systematic review and meta-analysis of a diagnostic test. *J Thromb Haemost*. 2019;17(5):787-794.
4. van Leeuwen EF, van der Ven JT, Engelfriet CP, von dem Borne AE. Specificity of autoantibodies in autoimmune thrombocytopenia. *Blood*. 1982;59(1):23-26.
5. McMillan R, Tani P, Millard F, Berchtold P, Renshaw L, Woods VL Jr. Platelet-associated and plasma anti-glycoprotein autoantibodies in chronic ITP. *Blood*. 1987;70(4):1040-1045.
6. Kiefel V, Santoso S, Kaufmann E, Mueller-Eckhardt C. Autoantibodies against platelet glycoprotein Ib/IX: a frequent finding in autoimmune thrombocytopenic purpura. *Br J Haematol*. 1991;79(2):256-262.
7. Singh A, Uzun G, Bakchoul T. Primary Immune Thrombocytopenia: Novel Insights into Pathophysiology and Disease Management. *J Clin Med*. 2021;10(4):789.
8. Li J, van der Wal DE, Zhu G, et al. Desialylation is a mechanism of Fc-independent platelet clearance and a therapeutic target in immune thrombocytopenia. *Nat Commun*. 2015;6:7737.
9. Marini I, Zlamal J, Faul C, et al. Autoantibody-mediated desialylation impairs human thrombopoiesis and platelet lifespan. *Haematologica*. 2021;106(1):196-207.
10. Zheng SS, Ahmadi Z, Leung HHL, et al. Antiplatelet antibody predicts platelet desialylation and apoptosis in immune thrombocytopenia. *Haematologica*. 2022;107(9):2195-2205.
11. Go RS, Johnston KL, Bruden KC. The association between platelet autoantibody specificity and response to intravenous immunoglobulin G in the treatment of patients with immune thrombocytopenia. *Haematologica*. 2007;92(2):283-284.
12. Zeng Q, Zhu L, Tao L, et al. Relative efficacy of steroid therapy in immune thrombocytopenia mediated by anti-platelet GPIIb/IIIa versus GPIIb/IIIa antibodies. *Am J Hematol*. 2012;87(2):206-208.
13. Peng J, Ma SH, Liu J, et al. Association of autoantibody specificity and response to intravenous immunoglobulin G therapy in immune thrombocytopenia: a multicenter cohort study. *J Thromb Haemost*. 2014;12(4):497-504.
14. Tao L, Zeng Q, Li J, et al. Platelet desialylation correlates with efficacy of first-line therapies for immune thrombocytopenia. *J Hematol Oncol*. 2017;10(1):46.
15. Shao L, Wu Y, Zhou H, et al. Successful treatment with oseltamivir phosphate in a patient with chronic immune thrombocytopenia positive for anti-GPIIb/IX autoantibody. *Platelets*. 2015;26(5):495-497.
16. Revilla N, Corral J, Minano A, et al. Multirefractory primary immune thrombocytopenia; targeting the decreased sialic acid content. *Platelets*. 2019;30(6):743-751.
17. Grodziński M, Goette NP, Glembotsky AC, et al. Multiple concomitant mechanisms contribute to low platelet count in patients with immune thrombocytopenia. *Sci Rep*. 2019;9(1):2208.
18. Woods VL Jr, Oh EH, Mason D, McMillan R. Autoantibodies against the platelet glycoprotein IIb/IIIa complex in patients with chronic ITP. *Blood*. 1984;63(2):368-375.
19. Kiefel V, Santoso S, Weisheit M, Mueller-Eckhardt C. Monoclonal antibody--specific immobilization of platelet antigens (MAIPA): a new tool for the identification of platelet-reactive antibodies. *Blood*. 1987;70(6):1722-1726.

20. Metzner K, Bauer J, Ponzi H, Ujcich A, Curtis BR. Detection and identification of platelet antibodies using a sensitive multiplex assay system-platelet antibody bead array. *Transfusion*. 2017;57(7):1724-1733.
21. Fujisawa K, O'Toole TE, Tani P, et al. Autoantibodies to the presumptive cytoplasmic domain of platelet glycoprotein IIIa in patients with chronic immune thrombocytopenic purpura. *Blood*. 1991;77(10):2207-2213.
22. Fujisawa K, Tani P, O'Toole TE, Ginsberg MH, McMillan R. Different specificities of platelet-associated and plasma autoantibodies to platelet GPIIb-IIIa in patients with chronic immune thrombocytopenic purpura. *Blood*. 1992;79(6):1441-1446.
23. Szatkowski NS, Kunicki TJ, Aster RH. Identification of glycoprotein Ib as a target for autoantibody in idiopathic (autoimmune) thrombocytopenic purpura. *Blood*. 1986;67(2):310-315.
24. Zhang N, Santoso S, Aster RH, Curtis BR, Newman PJ. Bioengineered iPSC-derived megakaryocytes for the detection of platelet-specific patient alloantibodies. *Blood*. 2019;134(22):e1-e8.
25. Quach ME, Li R. Structure-function of platelet glycoprotein Ib-IX. *J Thromb Haemost*. 2020;18(12):3131-3141.
26. Kanaji T, Russell S, Ware J. Amelioration of the macrothrombocytopenia associated with the murine Bernard-Soulier syndrome. *Blood*. 2002;100(6):2102-2107.
27. Li CQ, Dong JF, Lanza F, Sanan DA, Sae-Tung G, Lopez JA. Expression of platelet glycoprotein (GP) V in heterologous cells and evidence for its association with GP Ib alpha in forming a GP Ib-IX-V complex on the cell surface. *J Biol Chem*. 1995;270(27):16302-16307.
28. Strassel C, Moog S, Baas MJ, Cazenave JP, Lanza F. Biosynthesis of platelet glycoprotein V expressed as a single subunit or in association with GPIb-IX. *Eur J Biochem*. 2004;271(18):3671-3677.
29. Eksteen M, Tiller H, Averina M, et al. Characterization of a human platelet antigen-1a-specific monoclonal antibody derived from a B cell from a woman alloimmunized in pregnancy. *J Immunol*. 2015;194(12):5751-5760.
30. Lin M, Shieh SH, Liang DC, Yang TF, Shibata Y. Neonatal alloimmune thrombocytopenia in Taiwan due to an antibody against a labile component of HPA-3a (Baka). *Vox Sang*. 1995;69(4):336-340.
31. Harrison CR, Curtis BR, McFarland JG, Huff RW, Aster RH. Severe neonatal alloimmune thrombocytopenia caused by antibodies to human platelet antigen 3a (Bak^a) detectable only in whole platelet assays. *Transfusion*. 2003;43(10):1398-1402.
32. Kataoka S, Kobayashi H, Chiba K, et al. Neonatal alloimmune thrombocytopenia due to an antibody against a labile component of human platelet antigen-3b (Bak b). *Transfus Med*. 2004;14(6):419-423.
33. Barba P, Pallares P, Nogues N, et al. Post-transfusion purpura caused by anti-HPA-3a antibodies that are only detectable using whole platelets in the platelet immunofluorescence test. *Transfus Med*. 2010;20(3):200-202.
34. He R, Reid DM, Jones CE, Shulman NR. Extracellular epitopes of platelet glycoprotein Ib alpha reactive with serum antibodies from patients with chronic idiopathic thrombocytopenic purpura. *Blood*. 1995;86(10):3789-3796.
35. Zhou J, Xu Y, Shu J, et al. GPIbalpha CAAR-T cells function like a Trojan horse to eliminate autoreactive B cells to treat immune thrombocytopenia. *Haematologica*. 2024;109(7):2256-2270.
36. Varon D, Linder S, Gembom E, et al. Human monoclonal antibody derived from an autoimmune thrombocytopenic purpura patient, recognizing an intermediate filament's determinant common to vimentin and desmin. *Clin Immunol Immunopathol*. 1990;54(3):454-468.
37. Tomiyama Y, Kekomaki R, McFarland J, Kunicki TJ. Antivinculin antibodies in sera of patients with immune thrombocytopenia and in sera of normal subjects. *Blood*. 1992;79(1):161-168.

38. He R, Reid DM, Jones CE, Shulman NR. Spectrum of Ig classes, specificities, and titers of serum antiglycoproteins in chronic idiopathic thrombocytopenic purpura. *Blood*. 1994;83(4):1024-1032.
39. van Vliet HH, Kappers-Klunne MC, Abels J. Pseudothrombocytopenia: a cold autoantibody against platelet glycoprotein GP IIb. *Br J Haematol*. 1986;62(3):501-511.
40. Nugent DJ, Kunicki TJ, Berglund C, Bernstein ID. A human monoclonal autoantibody recognizes a neoantigen on glycoprotein IIIa expressed on stored and activated platelets. *Blood*. 1987;70(1):16-22.
41. Denomme GA, Smith JW, Kelton JG, Bell DA. A human monoclonal autoantibody to platelet glycoprotein IIb derived from normal human lymphocytes. *Blood*. 1992;79(2):447-451.
42. Kekomaki R, Dawson B, McFarland J, Kunicki TJ. Localization of human platelet autoantigens to the cysteine-rich region of glycoprotein IIIa. *J Clin Invest*. 1991;88(3):847-854.
43. Moroi M, Jung SM, Okuma M, Shinmyozu K. A patient with platelets deficient in glycoprotein VI that lack both collagen-induced aggregation and adhesion. *J Clin Invest*. 1989;84(5):1440-1445.
44. Boylan B, Chen H, Rathore V, et al. Anti-GPVI-associated ITP: an acquired platelet disorder caused by autoantibody-mediated clearance of the GPVI/FcRgamma-chain complex from the human platelet surface. *Blood*. 2004;104(5):1350-1355.
45. Gardiner EE, Al-Tamimi M, Mu FT, et al. Compromised ITAM-based platelet receptor function in a patient with immune thrombocytopenic purpura. *J Thromb Haemost*. 2008;6(7):1175-1182.
46. Rabbolini DJ, Gardiner EE, Morel-Kopp MC, et al. Anti-glycoprotein VI mediated immune thrombocytopenia: An under-recognized and significant entity? *Res Pract Thromb Haemost*. 2017;1(2):291-295.
47. Harrison C. CAR-Ts sweep into autoimmunity. *Nat Biotechnol*. 2024;42(7):995-997.
48. Ellebrecht CT, Bhoj VG, Nace A, et al. Reengineering chimeric antigen receptor T cells for targeted therapy of autoimmune disease. *Science*. 2016;353(6295):179-184.
49. Oh S, Mao X, Manfredo-Vieira S, et al. Precision targeting of autoantigen-specific B cells in muscle-specific tyrosine kinase myasthenia gravis with chimeric autoantibody receptor T cells. *Nat Biotechnol*. 2023;41(9):1229-1238.
50. Reincke SM, von Wardenburg N, Homeyer MA, et al. Chimeric autoantibody receptor T cells deplete NMDA receptor-specific B cells. *Cell*. 2023;186(23):5084-5097.

Figure Legends

Figure 1. Characterization of surface antigen levels in glycoprotein (GP)-deficient megakaryocytes (MK). (A) Flow cytometric analysis demonstrating the loss of surface expression of GPIIb-IIIa, but not α V β 3 and other major platelet surface glycoproteins, in GPIIb knockout MK. The schematic illustration on the left shows integrin β 3 (GPIIIa) pairs with either α IIb (GPIIb) or α V to form complexes on the MK surface. α V β 3 expression is detected with a complex-specific monoclonal antibody LM609. (B) Flow cytometric analysis of the surface expression of individual component in GPIb/IX/V complex in each GP knockout MK. The schematic illustration on the left shows that the chimeric IL4R α -GPIb α replaces most of the GPIb α extracellular domain (residues 1-472) with the interleukin-4 receptor α chain (IL4R α) extracellular domain (residues 1-198). The red line represents the disulfide bond formed between GPIb α and GPIb β . Color-coded numbers indicate the median fluorescence intensity of the corresponding peaks. ISO: isotype control for the staining antibody. WT: wild-type. KO: knockout.

Figure 2. Detection and characterization of anti-GPIIb-IIIa autoantibodies from ITP patient plasmas using whole megakaryocytes (WMK). The WT and GP-deficient MK were incubated with plasma from normal healthy controls or ITP patients. The MK-bound antibodies were detected with PE-conjugated donkey anti-human IgG using flow cytometry. Color-coded numbers indicate the median fluorescence intensity of the corresponding peaks. Autoantibodies detected by diagnostic antigen capture assay (ACA) and WMK in each patient's plasma are shown above the corresponding flow cytometry plots for comparison. (A) WMK detected anti-GPIIb-IIIa antibodies from ITP patient plasmas that had been previously confirmed with ACA in clinical diagnostic lab. A normal plasma is shown as a representative for negative controls. Anti-HPA-1a (26.4) antibody is a GPIIIa-specific human alloantibody. (B) WMK detected anti-GPIIb-IIIa antibodies from ITP patient plasmas that were previously undetectable with diagnostic ACA.

Figure 3. Detection and characterization of anti-GPIb/IX autoantibodies from ITP patient plasmas using whole megakaryocytes (WMK). The WT and GP-deficient MK were incubated with ITP patient plasma or a mixture of normal human plasma from 20 healthy donors. The MK-bound antibodies were detected by PE-conjugated donkey anti-human IgG with flow cytometry. Color-coded numbers indicate the median fluorescence intensity of the corresponding peaks. Autoantibodies detected by antigen capture assay (ACA) and WMK in each patient's plasma are shown above the corresponding flow cytometry plots for comparison. (A) WMK detected anti-GPIb/IX autoantibodies from ITP patient plasmas that had been confirmed with ACA in clinical diagnostic lab. WMK detected a strong anti-GPIb/IX antibody in patient 9, weak anti-GPIb/IX antibodies in patients 11 and 12, and a unique strong anti-GPIX antibody coexisting with a relatively weak anti-GPIIb-IIIa antibody in patient 10. (B) WMK detected anti-GPIb/IX autoantibodies from ITP patient plasmas that were previously undetectable with clinical ACA. WMK detected weak anti-GPIb/IX antibodies coexisting with strong anti-GPIIb-IIIa antibodies

in patients 13 to 15, and a strong anti-GPIb/IX antibody coexisting with a strong anti-GPIIb-IIIa antibody in patient 16.

Figure 4. Discrimination of non-membrane-reactive autoantibodies using whole megakaryocytes (WMK). (A) Comparison of WMK and clinical antigen capture assay (ACA) in detecting antiplatelet autoantibodies from ITP plasmas. As shown in *Supplementary Table S1*, blue indicates the cases that the WMK result matches the patient's lab ACA result. Orange indicates the cases that the patient's plasma autoantibody is detectable only with WMK, but not ACA. Pink indicates cases where at least one of the patient's plasma autoantibodies identified by ACA is not detected by WMK. (B) Clinical platelet antibody bead array (PABA) test of plasma from patient-17 showed strong reactivity to the GPIb/IX complex. Platelets from six individual donors were used in the testing panel. Data show the median fluorescence intensity of anti-human IgG detected from beads conjugated with MBC143.1 (anti-HLA class I), AP2 (anti-GPIIb/IIIa) and MBC142.17 (anti-GPIb/IX) antibodies. (C) WMK detected no platelet-reactive antibodies in the plasma from patient-17. (D) ACA using iPSC-derived MK demonstrates that the epitope recognized by patient-17's antibody is located on or associated with the extracellular domain of GPIb α . The GPIb/IX complex was captured from WT MK by anti-GPIb α monoclonal antibody MBC142.17. The IL4R α -GPIb/IX complex was captured from IL4R α -GPIb α MK by anti-IL4R α monoclonal antibody clone 25463. Autoantibody binding to the captured antigens was detected by horseradish peroxidase-conjugated anti-human IgG. OD: optical density. Values represent the means \pm SD from two independent experiments. *P<0.05, **P<0.01 by one-way ANOVA with Dunnett's test compared with normal plasma binding.

Figure 1

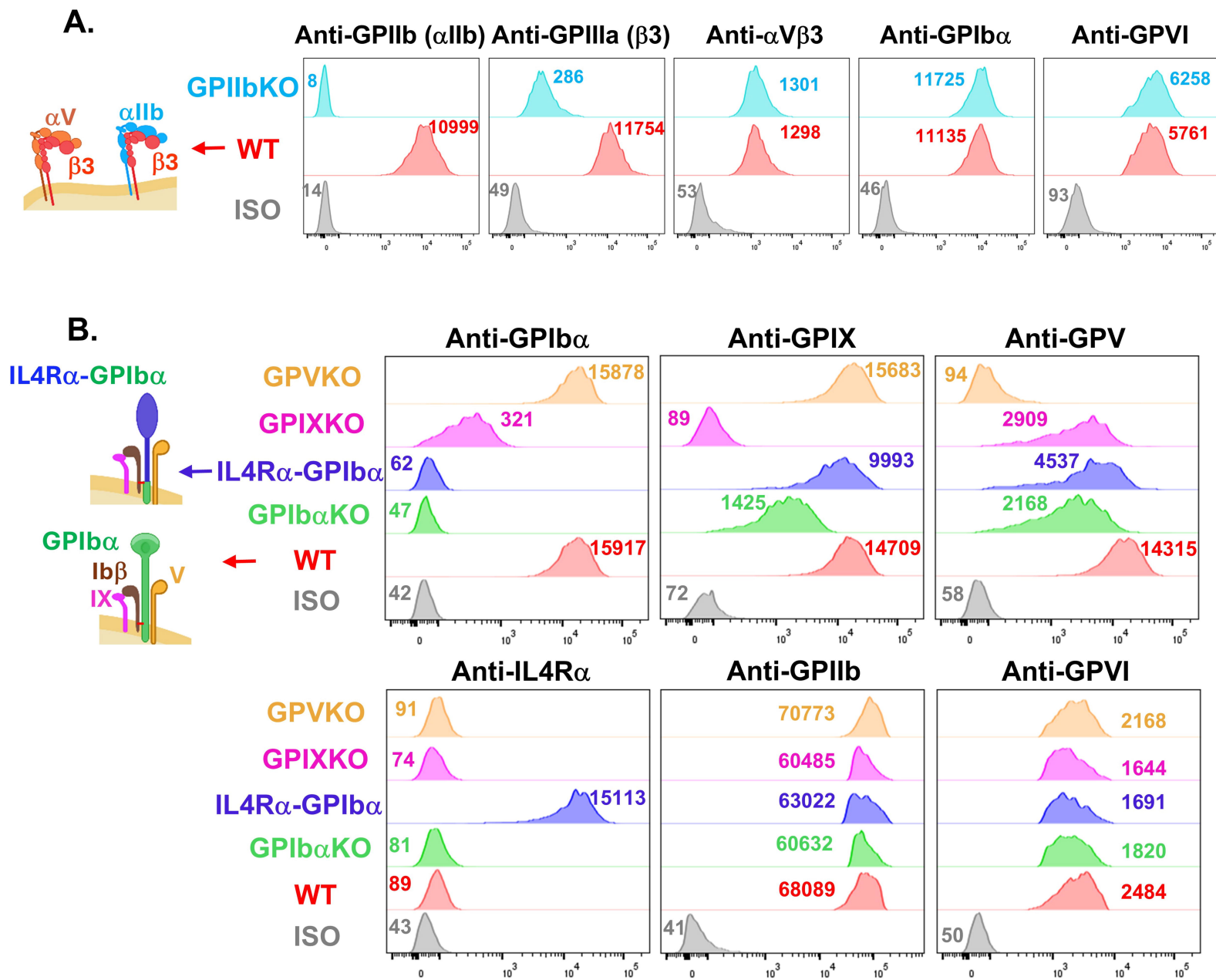


Figure 2

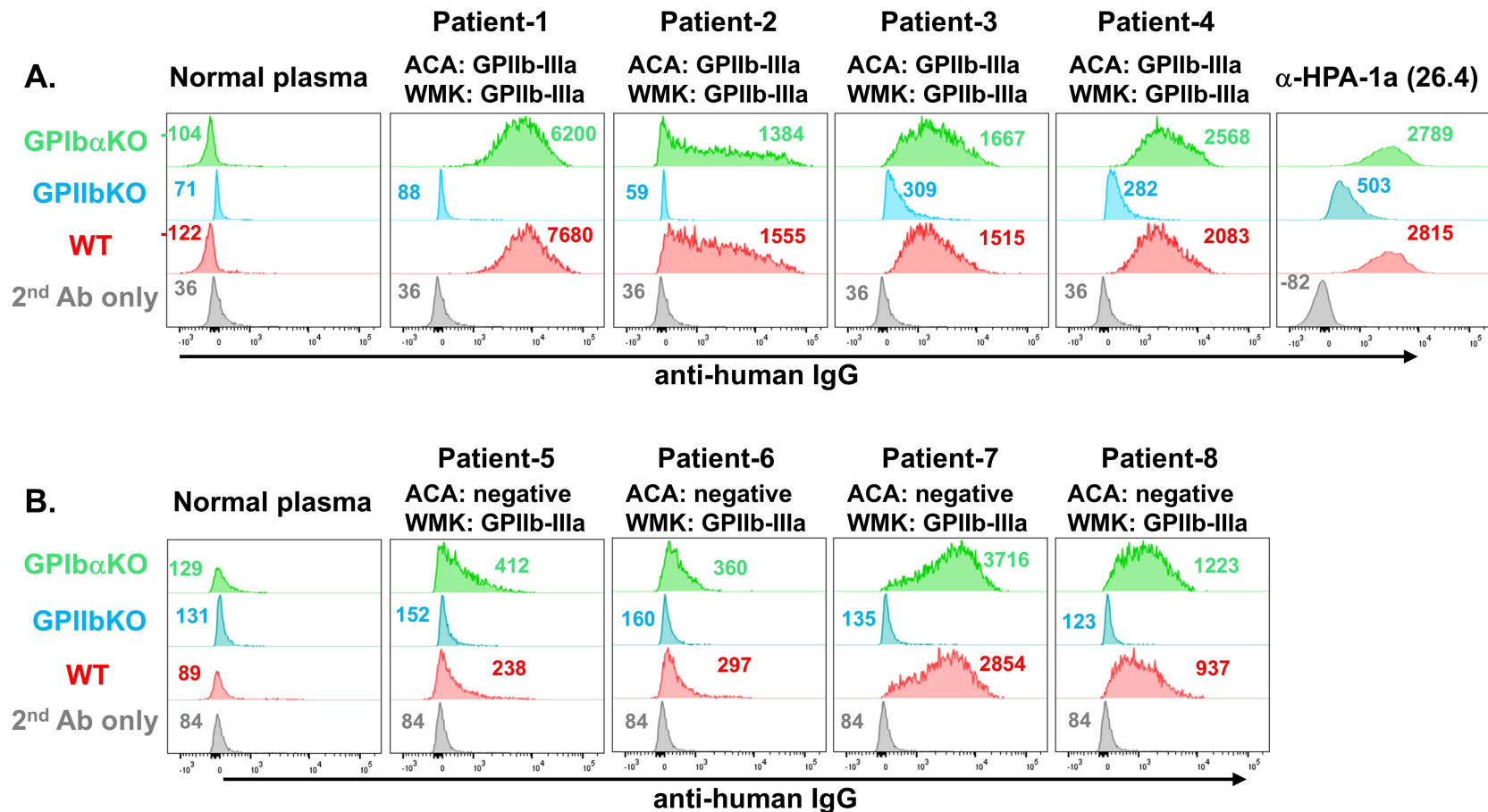


Figure 3

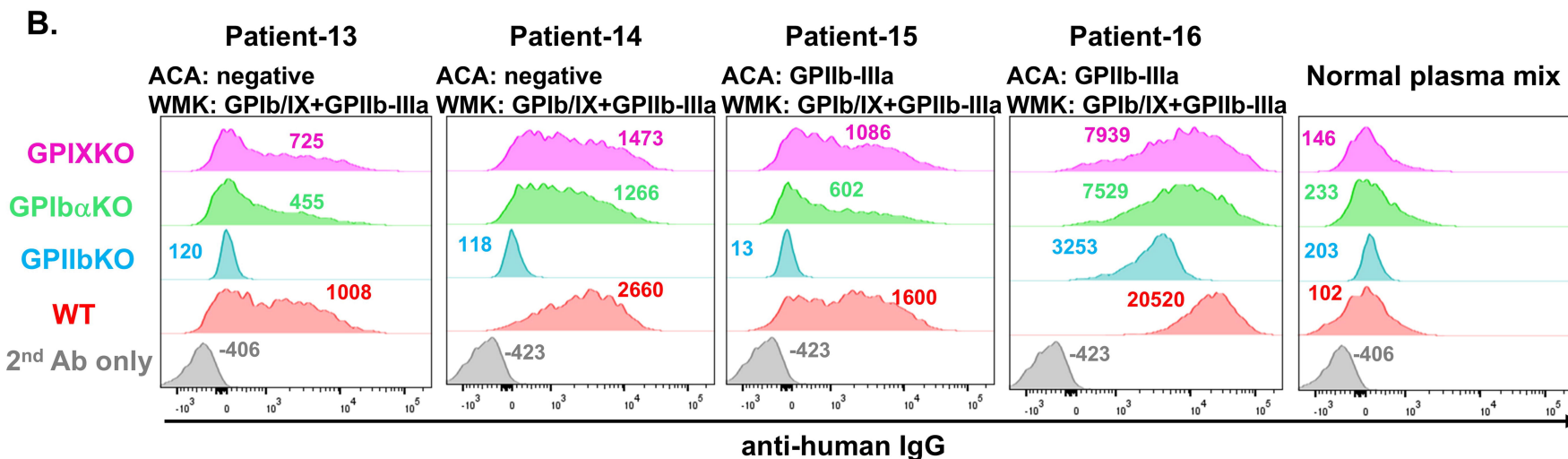
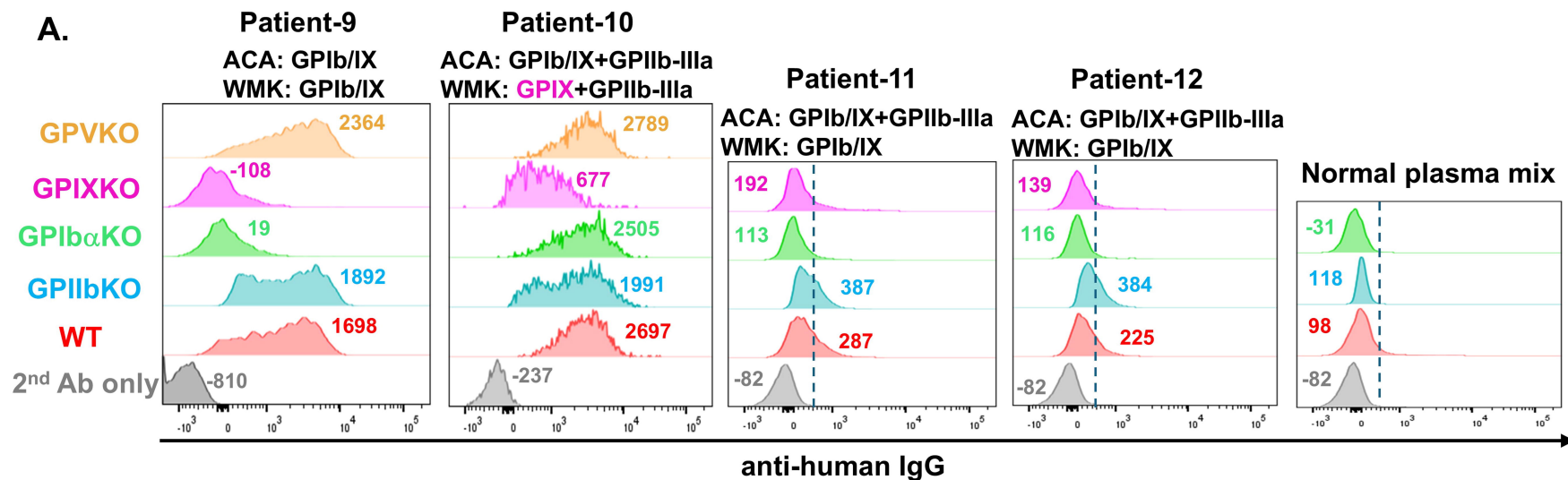
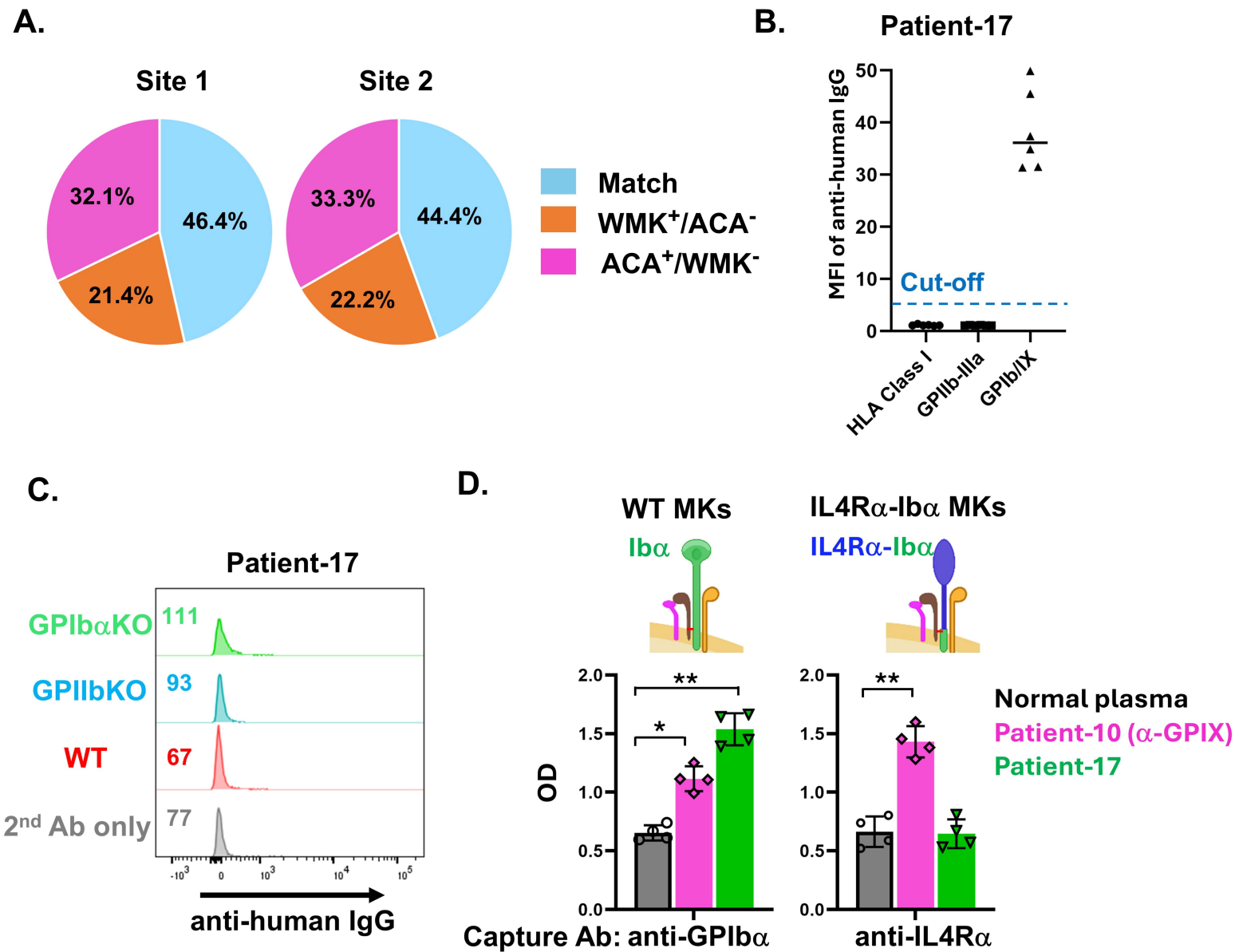


Figure. 4



Title

Differentiating pathogenic from bystander autoantibodies in immune thrombocytopenia
using intact glycoprotein-deficient megakaryocytes

Authors

Nanyan Zhang, Günalp Uzun, Tamam Bakchoul, Brian R. Curtis, and Peter J. Newman

Supplemental Materials




Table S1: ITP patient autoantibody testing results.

		Site 1 diagnostic test						Site 2 diagnostic test					
		Platelet Eluates		Plasma ACA				Plasma WМК					
		IІb-IIIa	Ib/IX	IІb-IIIa	Ib/IX			IІb-IIIa	Ib/IX	IІb-IIIa	Ib/IX		
PABA	Patient ID					MAIPA	Patient ID						
	Patient-1	NT	NT	pos	neg		Patient-11	pos	pos	pos	pos	neg	pos
	Patient-2	NT	NT	pos	neg		Patient-12	pos	pos	pos	pos	neg	pos
	Patient-3	pos	pos	pos	neg		Patient-13	pos	pos	neg	neg	pos	pos
	Patient-4	NT	NT	pos	neg		Patient-14	pos	pos	neg	neg	pos	pos
	Patient-5	pos	pos	neg	neg		Patient-15	pos	pos	pos	neg	pos	pos
	Patient-6	pos	pos	neg	neg		Patient-16	pos	pos	pos	neg	pos	pos
	Patient-7	pos	pos	neg	neg		Patient-18	pos	pos	pos	neg	pos	neg
	Patient-8	pos	pos	neg	neg		Patient-19	neg	pos	neg	neg	neg	neg
	Patient-9	NT	NT	neg	pos		Patient-20	pos	pos	neg	neg	neg	neg
	Patient-10	NT	NT	pos	pos		Patient-21	pos	pos	neg	neg	neg	neg
	Patient-17	NT	NT	neg	pos		Patient-22	pos	pos	pos	neg	pos	neg
	Patient-32	NT	NT	pos	neg		Patient-23	pos	pos	pos	neg	pos	neg
ELISA	Patient-33	pos	pos	neg	neg		Patient-24	pos	pos	pos	pos	pos	pos
	Patient-34	NT	NT	pos	neg		Patient-25	pos	pos	pos	pos	pos	pos
	<i>Patient-35</i>	pos	pos	pos	neg		Patient-26	neg	pos	neg	pos	pos	neg
	<i>Patient-36</i>	pos	pos	pos	neg		Patient-27	pos	pos	pos	pos	pos	neg
	<i>Patient-37</i>	pos	pos	pos	neg		Patient-28	pos	pos	pos	pos	neg	neg
	<i>Patient-38</i>	pos	pos	pos	neg		Patient-29	pos	pos	pos	pos	pos	neg
	<i>Patient-39</i>	pos	pos	neg	neg		Patient-30	pos	pos	pos	pos	neg	neg
	<i>Patient-40</i>	pos	pos	neg	neg		Patient-31	pos	pos	pos	pos	neg	neg
	<i>Patient-41</i>	pos	pos	neg	neg								
	<i>Patient-42</i>	pos	pos	neg	pos								
	<i>Patient-43</i>	pos	pos	neg	pos								
	<i>Patient-44</i>	pos	pos	neg	pos								
	<i>Patient-45</i>	pos	pos	pos	pos								
	<i>Patient-46</i>	pos	pos	pos	pos								
	<i>Patient-47</i>	pos	pos	pos	pos								
	<i>Patient-48</i>	pos	pos	neg	pos								

Match

WМК+/ACA-

ACA+/WМК-

 Match
 WMK⁺/ACA⁻
 ACA⁺/WMK⁻

Site 1 routinely uses ELISA to detect ITP autoantibodies in patient platelet eluates and plasma. The PABA test, equivalent to the well-known MACE test and more sensitive than ELISA, is often used when patients do not have sufficient platelets to prepare eluates. The top fourteen patient plasmas from Site 1 (patient IDs highlighted in **bold**) were tested with PABA. The bottom fourteen patient plasmas (patient IDs shown in *italics*) were tested with ELISA. Site 2 uses MAIPA to detect autoantibodies in patient platelet eluates and plasma. Results from the whole megakaryocyte (WMK) assay for detecting autoantibodies in patient plasmas are presented for comparison with lab plasma ACA testing. Blue indicates cases where the WMK result matches the patient's lab ACA result. Orange indicates cases where the patient's plasma autoantibody is detectable only with WMK but not ACA. Pink indicates cases where at least one of the patient's plasma autoantibodies identified by ACA is not detected by WMK. Two cases (patient 12 and 31) from Site 2 were treated with medication to reduce antibody production, which may have rendered the antibodies undetectable by WMK; these cases were not included in the comparison. **NT** indicates samples not tested due to insufficient platelet counts. **pos** stands for positive; **neg** stands for negative.

Table S2: gRNA sequences.

	Sequence from 5' to 3'
Guide 1 targeting <i>ITGA2B</i> gene	CAGCTGGAGCGACGTCATTG
Guide 2 targeting <i>ITGA2B</i> gene	GAGGCTGAGAAGACGCCCCGT
Guide 1 targeting <i>GPIBA</i> gene	TCTCACAGTTGCATAACCAG
Guide 2 targeting <i>GPIBA</i> gene	AAAGCCCATACAACCCCCTG
Guide 1 targeting <i>GPIX</i> gene	CCCATGTACCTGCCGCGCCC
Guide 2 targeting <i>GPIX</i> gene	AGGGGTTCTGCGTCACATCG
Guide 1 targeting <i>GPV</i> gene	GAGGGGGACTCTACTGTGCG
Guide 2 targeting <i>GPV</i> gene	TCACCCCTAAGTACCGCAGG
T2 guide targeting AAVS1 locus	GGGGCCACTAGGGACAGGAT

Table S3: PCR primers for genotyping.

	Sequence from 5' to 3'
ITGA2B-For	CTGGGATACGCTGGAATCTG
ITGA2B-Rev	GCTGGCGCTTACTAAAATCA
GPIBA-For	ACTCCAAGAGCTCTACCTGA
GPIBA-Rev	GGTCCATCTAGGTGGGAATG
GPIX-For	CTGGTTTCCCAGAGGAGAAG
GPIX-Rev	GCTGAGCTGCCAGTTTATTC
GPV-For	ATTCTGGCGAAAGGATTGTGCC
GPV-Rev	GCTGCTGAGATTGCGGAAGAG
AAVS1-For-1	TCGACTTCCCCTCTTCCGATG
AAVS1-Rev-1	CTCAGGTTCTGGGAGAGGGTAG
AAVS1-Rev-2	GGTCATTGGGCCAGGATTCTC
AAVS1-For-3	CAC TCGGAAGGACATATGGGAG
AAVS1-Rev-3	CCTGGGATACCCCGAAGAGT

Supplementary Figure 1

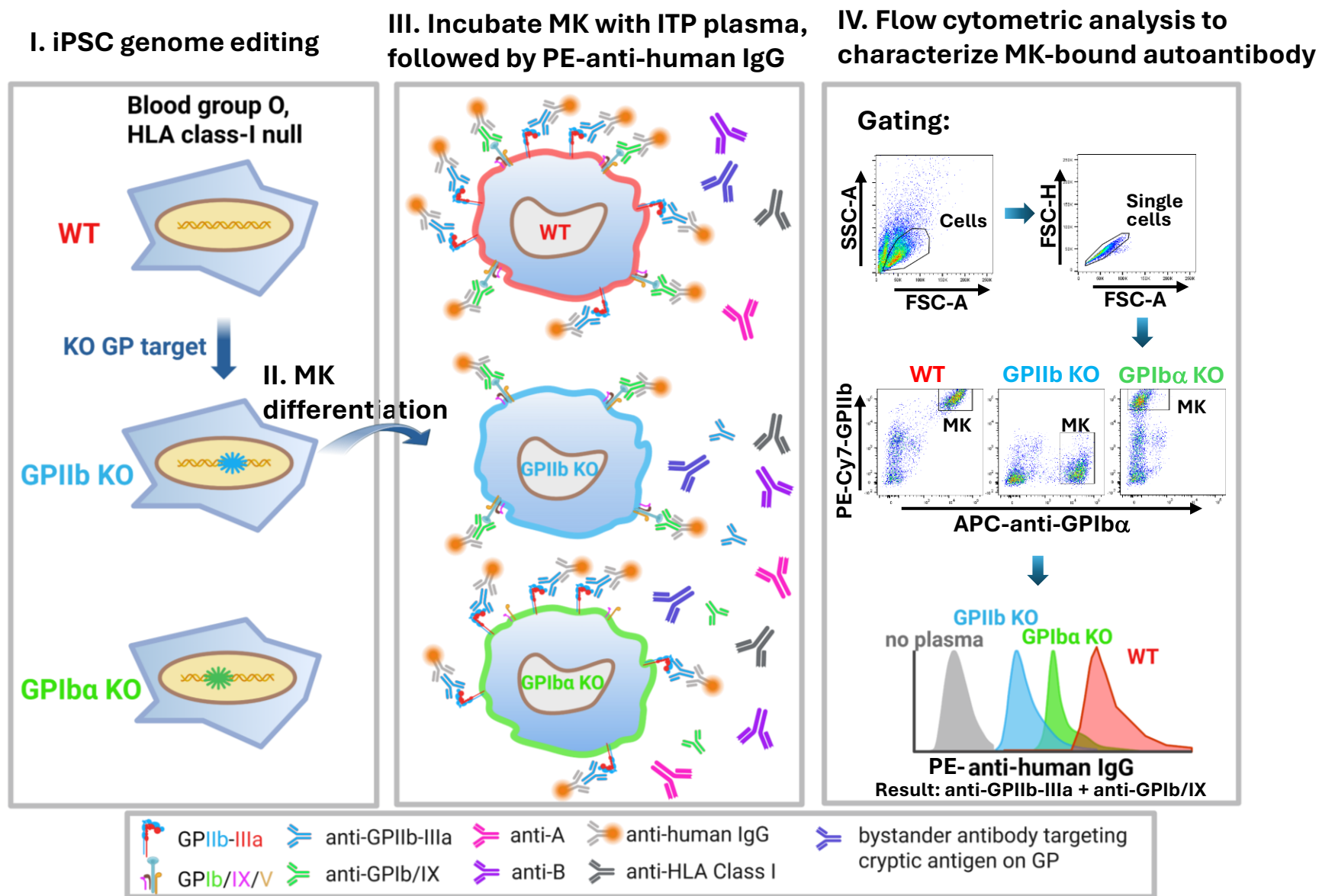


Figure S1. Workflow for detecting plasma autoantibodies in ITP using whole megakaryocytes. iPSC-derived MK can be cryopreserved and distributed to diagnostic laboratories for antibody testing.

Supplementary Figure 2

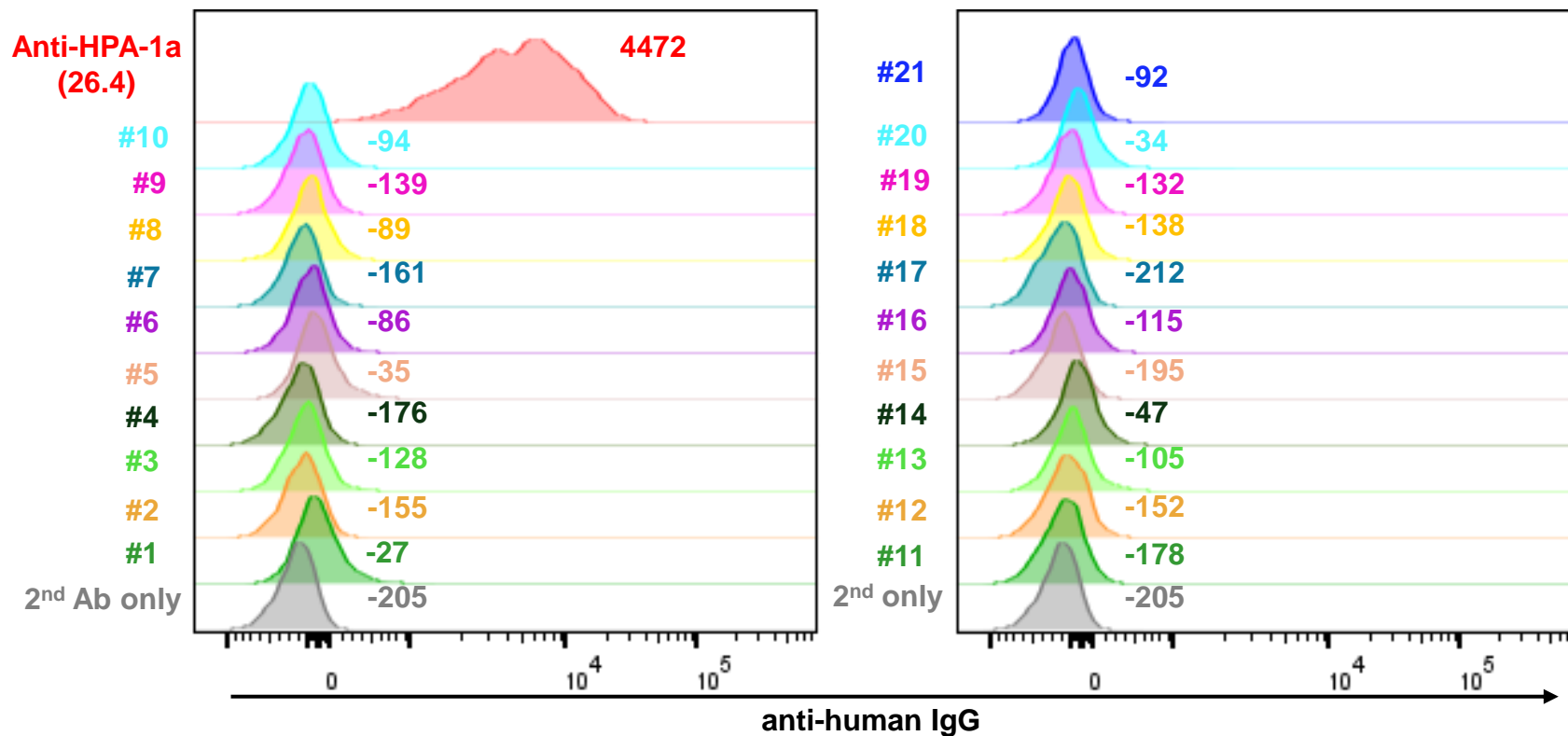


Figure S2. Low background binding of normal human plasmas to HLA class I-negative iPSC-derived MK. Twenty-one normal human plasma samples were tested with HLA class I-negative iPSC founder line-derived MK using flow cytometric analysis. Anti-HPA-1a (26.4) human antibody served as a positive control. MK-bound antibodies were detected with PE-conjugated donkey anti-human IgG. Color-coded numbers indicate the median fluorescence intensity of the corresponding peaks.

Supplementary Figure 3

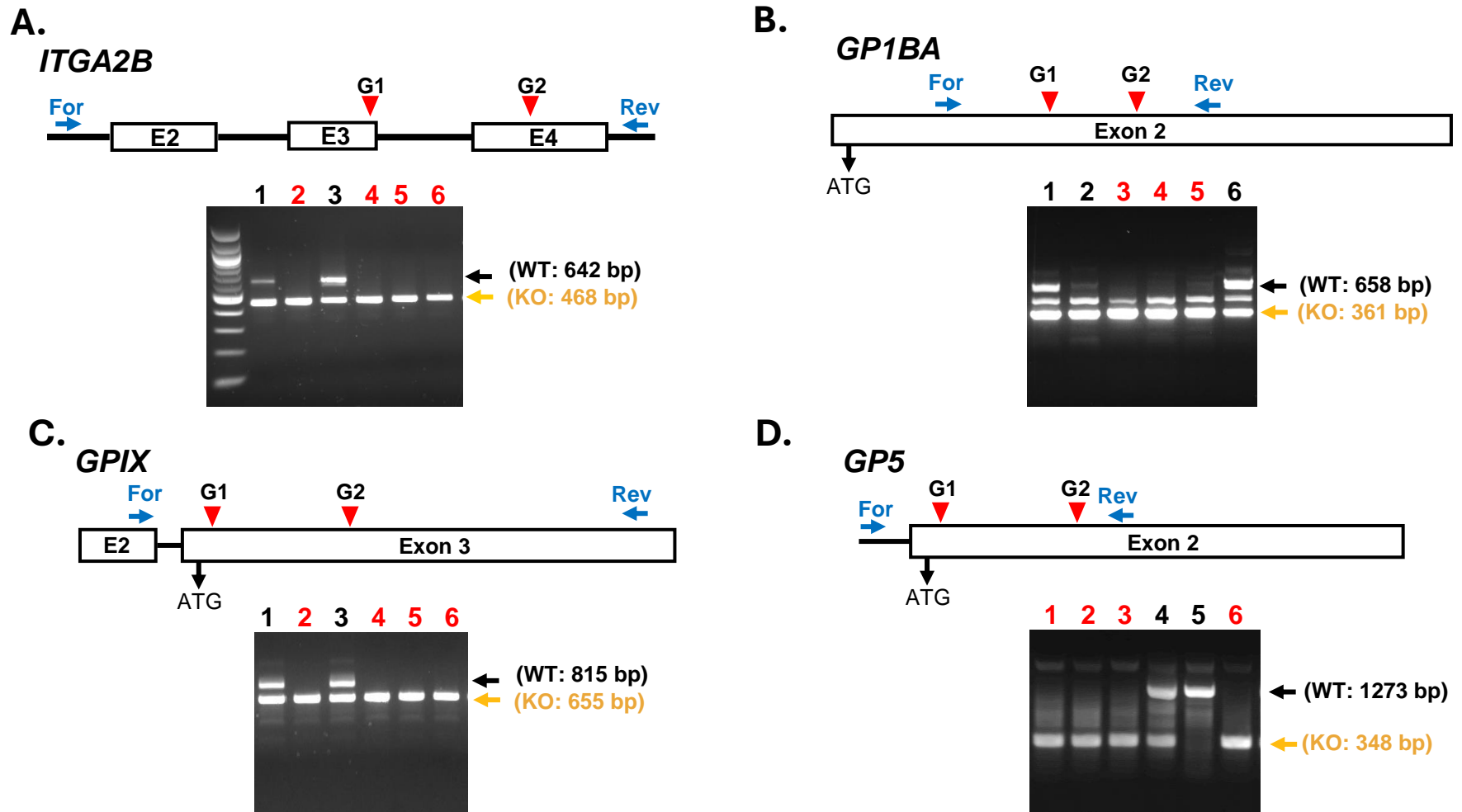


Figure S3. Generation of glycoprotein KO iPSC clones. Schematic representation of the *ITGA2B* (A), *GPIBA* (B), *GPIX* (C), and *GP5* (D) loci, illustrating the location of the gRNA binding sites (red arrowheads) and primer binding sites (blue arrows) for PCR genotyping. Genomic DNA from iPSC single clones, transfected with PX459 V2.0-gRNA1 and PX459 V2.0-gRNA2 targeting each respective gene, was PCR-amplified to screen for bi-allelic deletion at the targeted locus (highlighted in red). Black and orange arrows indicate the expected fragment sizes of the WT and KO alleles, respectively.

Supplementary Figure 4

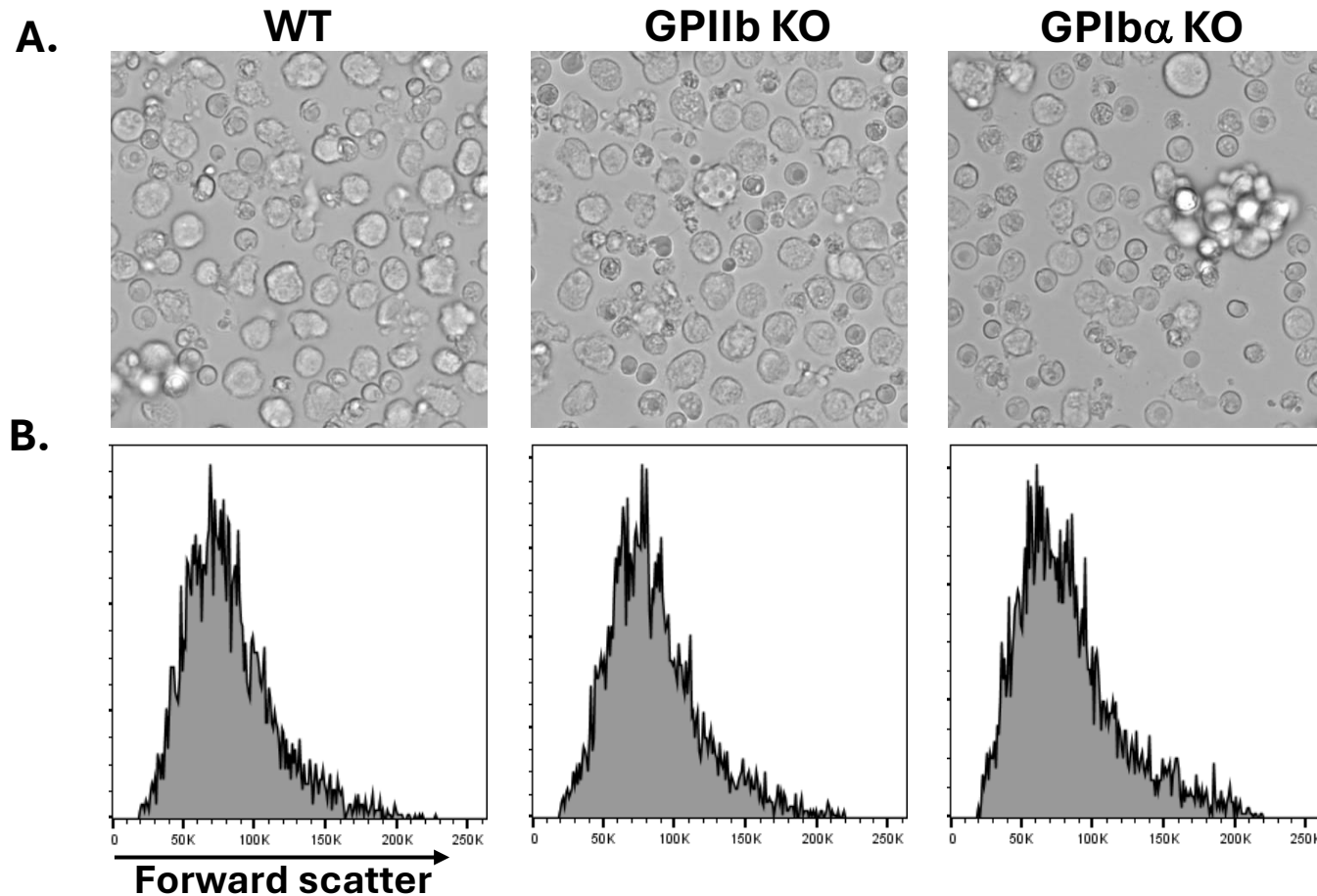
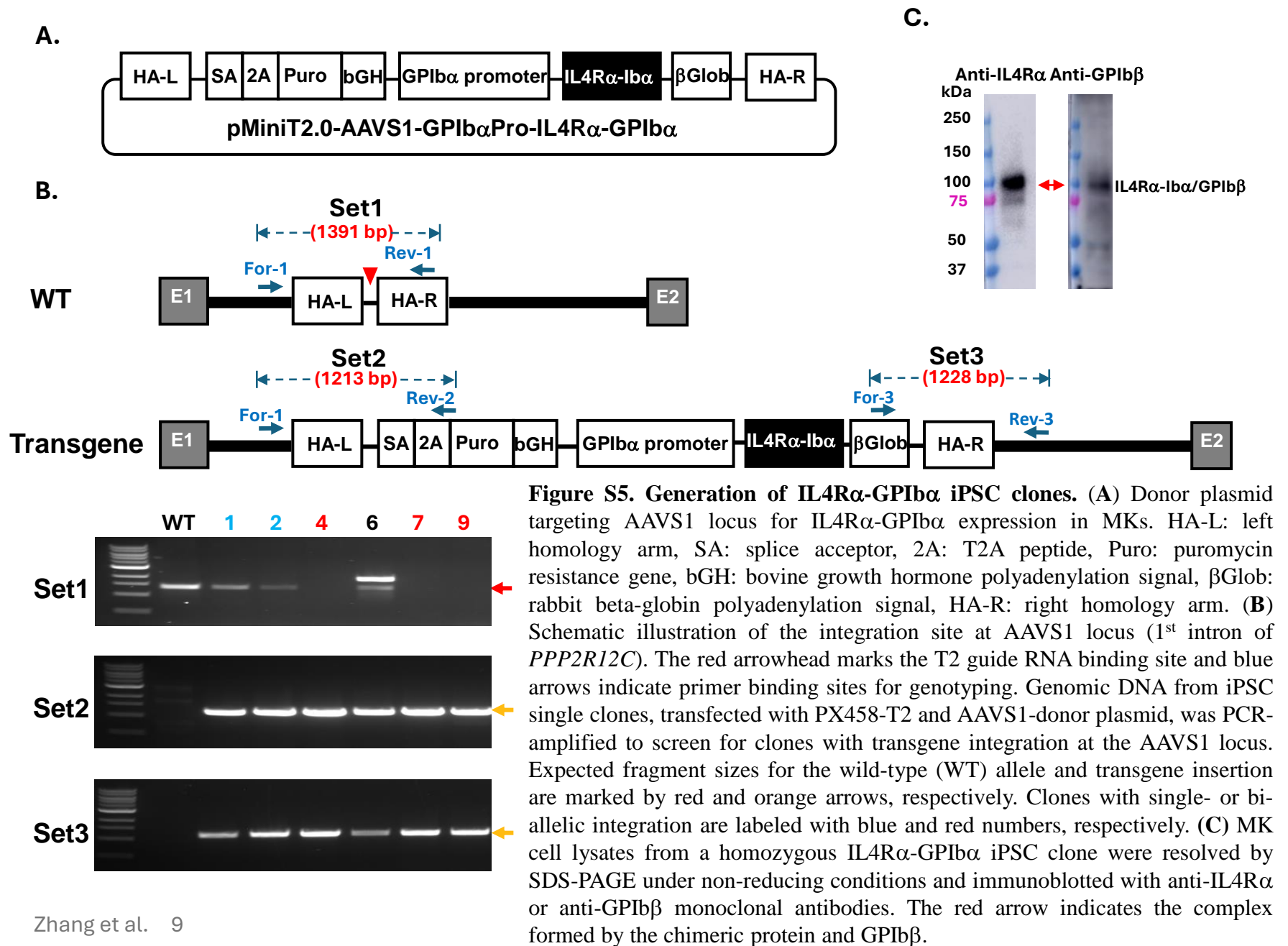


Figure S4. Normal size distribution of glycoprotein-deficient MK. (A) Representative images of iPSC-derived MK from various cell lines. (B) Flow cytometric analysis of iPSC-derived MK from different cell lines, comparing size distribution between GP KO and WT MKs.

Supplementary Figure 5



Supplemental Figure 6

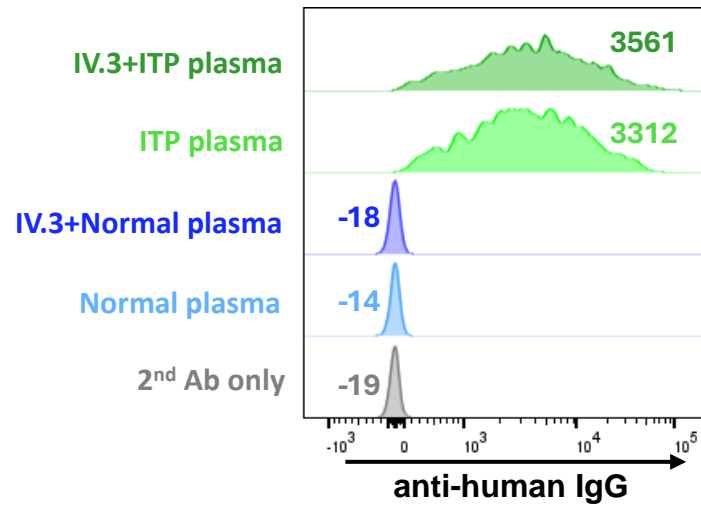


Figure S6. Blocking FcγRIIa receptors does not affect ITP autoantibody binding to iPSC-derived MKs. WT MKs were preincubated with 10 mg/ml anti-FcγRIIa antibody IV.3 for 20 min before being incubated with either normal human plasma or ITP plasma from Patient-2. The MK-bound autoantibodies were detected using PE-conjugated donkey anti-human IgG and analyzed by flow cytometry. Color-coded numbers indicate the median fluorescence intensity of the corresponding peaks.

Supplemental Figure 7

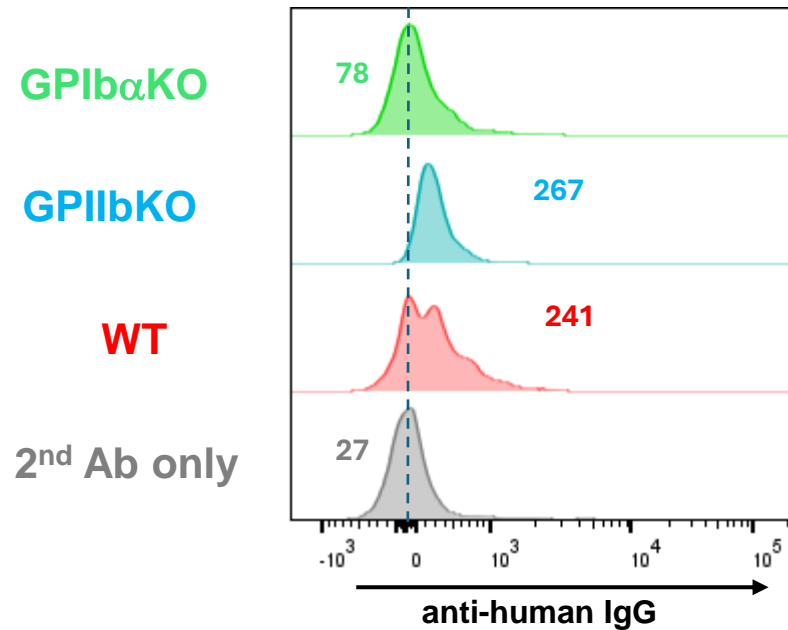


Figure S7. Detection of a missed anti-GPIb/IX antibody in the plasma of a Bernard–Soulier syndrome (BSS) patient using WMK. This BSS patient was suspected to harbor an anti-GPIb/IX antibody following prior blood transfusion. However, the antibody was not detected by the clinical diagnostic PABA test. In contrast, WMK successfully revealed a weak anti-GPIb/IX antibody in the patient’s plasma.

Supplementary Figure 8

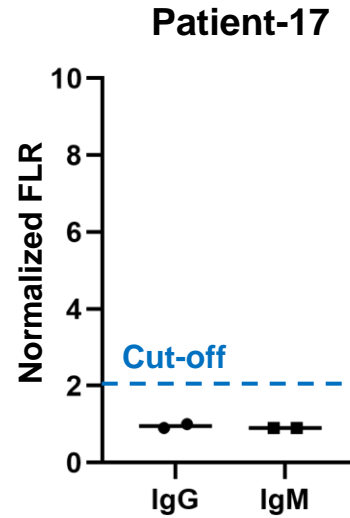


Figure S8. Lack of detectable antibody binding to intact platelets by plasma from patient-17. Plasma from patient-17 showed no antibody binding to human platelets from two individual donors in whole platelet flow cytometry. The cut-off for a positive in this standard clinical test is an FLR ≥ 2.0 .

Supplemental Figure 9

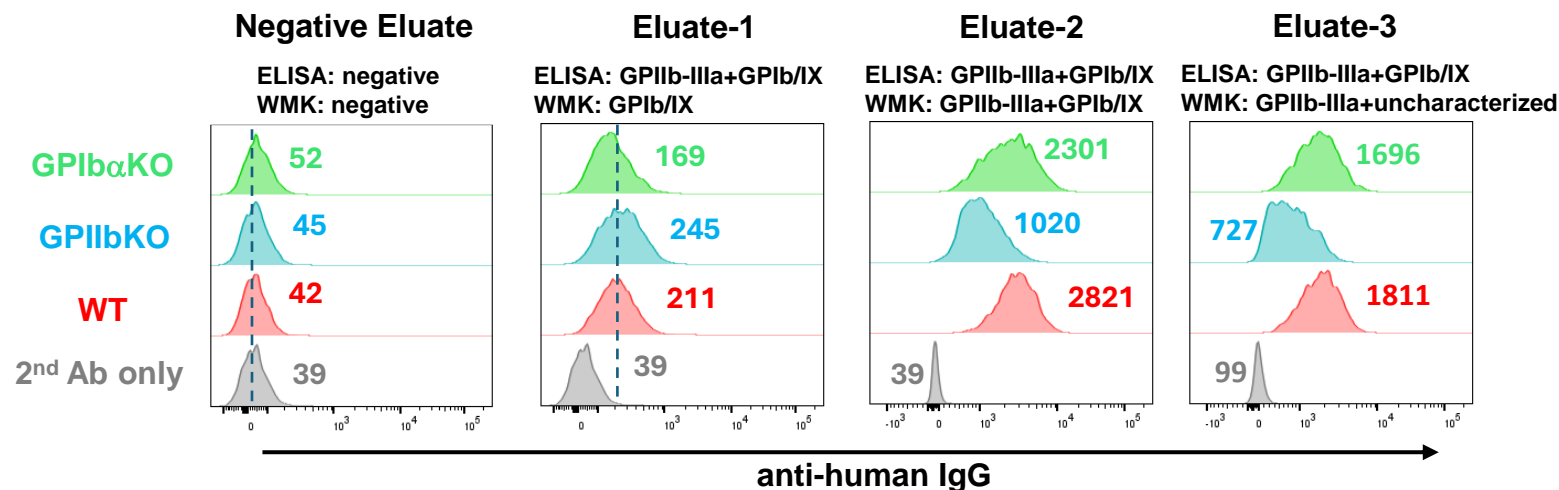


Figure S9. Detection and characterization of ITP autoantibodies in patient platelet eluates using WMK. Platelet eluates from three ITP patients with detectable autoantibodies in diagnostic ELISA were tested by WMK. In each reaction, 5×10^5 MKs were incubated with eluates prepared from 7.5×10^6 patient platelets. MK-bound antibodies were detected using PE-conjugated donkey anti-human IgG and analyzed by flow cytometry. Color-coded numbers indicate the median fluorescence intensity (MFI) of the corresponding peaks. Autoantibodies identified by diagnostic ELISA and by WMK in each patient's platelet eluate are shown above the corresponding flow cytometry plots for comparison. WMK detected weak anti-GPIb/IX autoantibodies in Eluate-1, coexistence of strong anti-GPIIb-IIIa and relatively weak anti-GPIb/IX antibodies in Eluate-2, and strong anti-GPIIb-IIIa antibodies along with an additional uncharacterized antibody in Eluate-3. Further testing with GPIX KO and GPVKO MK was not possible due to the limited availability of patient samples.

Supplemental methods

Guide RNA plasmid constructs

gRNAs targeting platelet surface glycoproteins GPIIb, GPIb α , GPIX and GPV were designed using the CRISPR Design Tool <https://benchling.com/crispr>. gRNA sequences are summarized in *Supplementary Table S2*. Oligos were cloned into the BbsI site of the Cas9 expression plasmids PX459 V2.0 (Addgene).

Generation of glycoprotein-deficient iPSC lines

B2M KO OT1-1 iPSCs¹ were maintained on Matrigel (Corning)-coated plates in StemFlex Medium (Thermo Fisher Scientific) at 37 °C with 4% O₂/5% CO₂. The iPSCs were incubated with 10 μ M Y27632 for 2 hours before transfection. To generate glycoprotein-deficient iPSC lines, 2x10⁵ cells were transfected with 1 μ g of guide plasmid pairs targeting individual gene, including *ITGA2B*, *GPIBA*, *GPIX* or *GPV* using the Amaxa P3 primary cell 4D Nucleofector Kit (Lonza) and Nucleofector Program CB-150. 24-hour post-transfection, 1 μ g/ml puromycin was applied for 48 hr. Single clones were harvested at 12 to 14 days post-puromycin-selection and replated on Matrigel-coated plates.

Generation of IL4R α -GPIb α iPSC line

T2 guide targeting AAVS1 locus was selected from previous research² and cloned into the BbsI site of PX458 plasmids (Addgene). To generate AAVS1 targeting donor plasmid (*Supplementary Figure S5*) for knocking-in transgene encoding IL4R α -GPIb α chimeric protein, a 1.7 kb gBlock gene fragment (Integrated DNA Technologies) containing AAVS1 homologous arms flanking a splicing acceptor and multiple cloning sites in the middle was first inserted into the XhoI/NotI site of pMiniT 2.0 vector. Three DNA fragments were then assembled into the multiple cloning sites using In-Fusion Snap Assembly EcoDry cloning kit (Takara Bio USA). The 1 kb fragment containing T2A, puromycin resistance gene followed by bovine growth hormone polyadenylation signal was amplified by polymerase chain reaction (PCR) from PX459 V2.0 plasmid. The 3.1 kb human GPIb α promoter cassette was amplified by PCR from pCDNAzeo-hGPIb α pro-hIL4R α -GPIb α plasmid,³ a kind gift from Dr. Taisuke Kanaji (The Scripps Research Institute, La Jolla, CA). The 1.4 kb gBlock Gene Fragment encoding IL4R α -GPIb α fusion protein followed by a rabbit beta-globin polyadenylation signal was synthesized by Integrated DNA Technologies.

To generate IL4R α -GPIb α iPSC line, 1x10⁶ GPIb α -deficient iPSC were co-transfected with 1 μ g of T2 guide plasmid and 3 μ g of AAVS1-IL4R α -GPIb α donor plasmid using the Amaxa P3 primary cell 4D Nucleofector Kit. 48-hour post-transfection 0.5 μ g/ml puromycin was applied for 48 hr. Single clones were harvested at 12 to 14 days post-puromycin-selection and replated on Matrigel-coated plates.

Genotyping

Genomic DNA was extracted from each iPSC clone using the QuickExtract DNA Extraction Solution (Epicenter) following the manufacture's instruction. The regions surrounding the targeted deletion of genes encoding corresponding glycoproteins or the transgene integration site at AAVS1 locus were amplified by PCR using the primers listed in *Supplementary Table S3*. PCR products were analyzed on 1% or 2% agarose gels.

Differentiation of iPSCs

CRISPR-edited iPSC lines were differentiated to MK as previously described^{4,5}. Briefly, cells were plated on Matrigel-coated 6-well plates and maintained at 37°C with 4% O₂/5% CO₂. Media and cytokine changes were followed as described for 9 days except that 1 μM of CHIR99021 (Tocris) was used instead of Wnt3a. Hematopoietic progenitor cells (HPC) in suspension or loosely attached to the bottom were collected by carefully removing the supernatant, then analyzed by flow cytometry to confirm surface expression of CD41 and CD235a. The HPC were further differentiated to MK at 37 °C, 5% CO₂ for 6 days in serum-free differentiation medium, a mixture of Iscove's Modified Dulbecco's Medium (Thermo Fisher Scientific) and Ham's F-12 (Corning) at 3:1 ratio, supplemented with 0.5% N2 (Thermo Fisher Scientific), 1% B27 without Vitamin A (Thermo Fisher Scientific), 0.05% BSA (Sigma), 2mM L-glutamine, 50 U/ml penicillin, 50 μg/ml streptomycin, 50 ng/ml SCF and 50 ng/ml TPO (R&D systems). MK were analyzed by flow cytometry to confirm the surface expression of CD41 and CD42b.

Antigen capture assay

To locate the epitope targeted by the antibody in patient-17's plasma, 5x10⁵ MK expressing either WT GPIb/IX or IL4Rα-Ib/IX complex were incubated with 50 μl of diluted normal human plasma or ITP patient plasma at room temperature for 1 hour. After three washes with TBS containing 1 mM CaCl₂, the cells were solubilized in TBS containing 0.1 mM CaCl₂, 1% Triton X-100 and protease inhibitor cocktail. After removing insoluble material by centrifugation at 20,000g for 30 minutes, the cell lysates were applied to a well of 96-well microplate that contains fixed mAb against either GPIbα (142.17) or IL-4Rα (25463). After 1 hour incubation, the plate was washed four times with TBS containing 0.1 mM CaCl₂, 0.1% Tween 20, and 3% BSA. Well-bound human antibodies were detected with horseradish peroxidase-conjugated donkey anti-human IgG and ultra TMB ELISA substrate solution. The reaction was stopped by addition of sulfuric acid, and the optical density (OD) was measured at 450 nm.

References

1. Zhang N, Santoso S, Aster RH, Curtis BR, Newman PJ. Bioengineered iPSC-derived megakaryocytes for the detection of platelet-specific patient alloantibodies. *Blood*. 2019;134(22):e1-e8.
2. Mali P, Yang L, Esvelt KM, et al. RNA-guided human genome engineering via Cas9. *Science*. 2013;339(6121):823-826.
3. Kanaji T, Russell S, Ware J. Amelioration of the macrothrombocytopenia associated with the murine Bernard-Soulier syndrome. *Blood*. 2002;100(6):2102-2107.
4. Mills JA, Paluru P, Weiss MJ, Gadue P, French DL. Hematopoietic differentiation of pluripotent stem cells in culture. In: Qu KDBaC-K, ed. *Methods in Molecular Biology*. New York: Springer Science+Business Media, 2014:181-194.
5. Paluru P, Hudock KM, Cheng X, et al. The negative impact of Wnt signaling on megakaryocyte and primitive erythroid progenitors derived from human embryonic stem cells. *Stem cell research*. 2014;12(2):441-451.